Probing the Conformational States of the SH1−SH2 Helix in Myosin: A Cross-Linking Approach †

ARTICLE *in* BIOCHEMISTRY · DECEMBER 1998

Impact Factor: 3.02 · DOI: 10.1021/bi9817212 · Source: PubMed

2 AUTHORS, INCLUDING:

Emil Reisler
University of California, Los Angeles
230 PUBLICATIONS **5,576** CITATIONS

SEE PROFILE

Probing the Conformational States of the SH1−SH2 Helix in Myosin: A Cross-Linking Approach†

Lisa K. Nitao and Emil Reisler*

Department of Chemistry and Biochemistry and Molecular Biology Institute, University of California, Los Angeles, California 90095

Received July 17, 1998; Revised Manuscript Received September 24, 1998

ABSTRACT: Previous biochemical studies have shown that the SH1 (Cys707) and SH2 (Cys697) groups on rabbit skeletal myosin subfragment 1 (S1) can be cross-linked by using reagents of different cross-linking lengths. In the presence of nucleotide, this cross-linking is accelerated. In the crystal structure of S1, the SH1 and SH2 residues are located on an α-helix, 19 Å apart. Thus, the cross-linking results could be indicative of helix melting or increased flexibility in the presence of nucleotides. Nucleotide-induced changes in this region were examined in this study by monitoring the cross-linking of SH1 and SH2 on S1 with dimaleimide reagents of spans ranging from 5 to 15 Å. A method was devised to directly measure the kinetic effects of nucleotides on the rates of cross-linking reactions. The slow and reagent-insensitive rates of the SH1−SH2 cross-linking in the absence of nucleotides reveal that the equipartitioning of the SH1−SH2 helix among states with different SH1−SH2 separations occurs infrequently. In the presence of MgADP, MgATP, and MgATPγS, the rates of SH1 and SH2 cross-linking were increased ∼2−7-fold for the shortest reagent (5−8 Å). Rate accelerations were much greater for the longer reagents (9−15 Å): 40−50-fold for MgADP, 25−40-fold for MgATP, and 80−270-fold for MgATPγS. To account for any nucleotide-dependent differences in the reactivities of the reagents toward SH2, the rates of monofunctional SH2 modification on SH1-labeled S1 were also measured for each reagent. These experiments showed that the nucleotide-induced increases in the rates of SH2 modification were similar for all of the reagents. Thus, the changes observed in the cross-linking rates are due not only to the type of nucleotide bound in the active site but also to the span of the cross-linking reagent. These findings are interpreted in terms of nucleotide-induced shifts in the equilibria among conformational states of the SH1−SH2 helix.

Myosin is a molecular motor that converts the chemical energy of ATP to mechanical work. For years, considerable effort has focused on how myosin functions. It is believed that ATP hydrolysis induces structural changes in the myosin head, which result in the directed movement of the actin filament. As ATP is hydrolyzed, different transitional states are created in the myosin head (*1*). These transitional states are associated with conformational changes that are necessary to transduce the chemical energy for force production. Recently, X-ray crystallographic structures of the myosin motor domain complexed with nucleotide and phosphate analogues were determined (*2*−*4*). When bound to myosin, these analogues represent both the prehydrolysis state (MgADP·BeF_x, MgATPγS, MgAMPPNP) and the post-hydrolysis state (MgADP·AlF_4^-, MgADP·VO_4). When the structures of these different states are compared, several regions of the motor domain appear to shift. A proposed mechanism for hydrolysis suggests that changes in these regions are transmitted to and then amplified by the light chain binding domain (*5*). Therefore, studies of these regions may reveal what structural changes are occurring in the myosin head as it converts the energy of ATP to motor function.

One site on myosin subfragment 1 (S1)[1] that has been of particular interest is the helix containing the reactive sulfhydryls, Cys707 (SH1) and Cys697 (SH2). The SH1−SH2 helix has been shown previously to undergo nucleotide-induced structural changes (*6*). A variety of reagents specifically modify and cross-link these two groups. In the presence of nucleotide, SH1 and SH2 can be cross-linked with reagents of spans ranging from 3 to 14 Å (*7*, *8*). Under certain conditions, a disulfide bond may even be formed between the two groups (*9*). From the atomic structure of the S1, these cysteine residues are located on opposite sides of a bent helix, and the distance between the sulfur atoms is approximately 19 Å (*10*). Therefore, in the presence of nucleotide, the helix must undergo some conformational changes in order for SH1 and SH2 to come close to each other. To account for these changes, two explanations can

† This work was supported by grants from USPHS National Research Service Award GM07185 (to L.K.N.) and USPHS AR22031 and NSF MCB-9630997.

[1] Abbreviations: ATPγS, adenosine 5′-(3-thiotriphosphate); BM, 1,1′-(methylenedi-4,1-phenylene)bismaleimide; mPDM, *N*,*N*′-1,3-phenylenedimaleimide; DTT, dithiothreitol; NDM, naphthalene-1,5-dimaleimide; NEM, *N*-ethylmaleimide; oPDM, *N*,*N*′-1,2-phenylenedimaleimide; pPDM, *N*,*N*′-1,4-phenylenedimaleimide; S1, myosin subfragment 1; SH1, Cys707 in the rabbit (or chicken) skeletal S1 sequence; SH2, Cys697 on S1.

10.1021/bi9817212 CCC: $15.00
Published on Web 11/01/1998

be suggested. Upon nucleotide binding, the helix may be collapsing or melting. Alternatively, the helix may be bending or have increased flexibility, which would then allow SH1 and SH2 to approach each other.

In previous cross-linking studies, the effect of nucleotides on the SH1−SH2 helix was estimated from results which had not separated SH1 modification and subsequent cross-linking activities (*11*, *12*). In this study, a scheme was devised to isolate the cross-linking reaction. With this scheme, the actual changes induced by nucleotide can be determined. Cross-linking reagents of different spans were utilized to probe the distance separating SH1 and SH2. The spans of the reagents range from approximately 5 Å for the shortest reagent (oPDM) to 15 Å for the longest reagent (BM). The effect of three nucleotide states, MgADP, MgATPγS, and MgATP, on the SH1−SH2 cross-linking was examined in this study. Our results show that the effect of nucleotide on the cross-linking rates depends on both the nucleotide state and the span of the cross-linking reagent. These results are discussed in terms of the nucleotide-induced flexibility of the SH1−SH2 helix.

MATERIALS AND METHODS

Reagents. *N*-Ethylmaleimide (NEM), ADP, and Sephadex G-50 were purchased from Sigma (St. Louis, MO). *N*,*N*′-1,2-Phenylenedimaleimide (oPDM) and *N*,*N*′-1,4-phenylenedimaleimide (pPDM) were from Research Organics (Cleveland, OH). *N*,*N*′-1,3-Phenylenedimaleimide (mPDM), naphthalene-1,5-dimaleimide (NDM), and 1,1′-(methylenedi-4,1-phenylene)bismaleimide (BM) were from Aldrich (Milwaukee, WI). Adenosine 5′-(3-thiotriphosphate) (ATPγS) was obtained from Boehringer Mannheim (Germany).

Determination of Cross-Linking Spans. Each cross-linking reagent was drawn in the ChemDraw program and transferred to the MacroModel program which used energy minimalization in determining the cross-linking distances for different conformers. The reagents and their cross-linking spans are shown in Figure 1.

Proteins. Myosin from rabbit psoas muscle was prepared according to Godfrey and Harrington (*13*). Subfragment 1 (S1) was prepared by chymotryptic digestion of myosin filaments as described by Weeds and Pope (*14*). The concentration of S1 was determined spectrophotometrically by using an extinction coefficient of $E1\%280 = 7.5\ cm^{-1}$.

ATPase Activities. Ca^{2+}- and EDTA- (K^+-)ATPase activities of S1 were determined at 37 °C according to Fiske and Subbarow (*15*). The Ca^{2+}-ATPase assay solution contained 600 mM KCl, 50 mM Tris-HCl (pH 7.6), 5.0 mM $CaCl_2$, and 2.0 mM ATP. The EDTA-ATPase assay solution contained 444 mM KCl, 50 mM histidine, 50 mM Tris-HCl (pH 7.6), 5.0 mM EDTA, and 2.0 mM ATP.

Cross-Linking Experiments. All cross-linking reactions were carried out in three steps. In the first step, bifunctional reagents were attached to SH1 on S1. This involved reacting the cross-linking reagent (18 μM) with S1 (12 μM) in 10 mM KCl, 10 mM imidazole, pH 7.0 at 4 °C. Because the oPDM reaction was much slower than the other reactions, 1.0 mM MgADP was included in the modification of SH1 by this reagent only. For all of the reactions, the conditions were chosen to optimize SH1 modification without significant SH1−SH2 cross-linking. The modification reactions

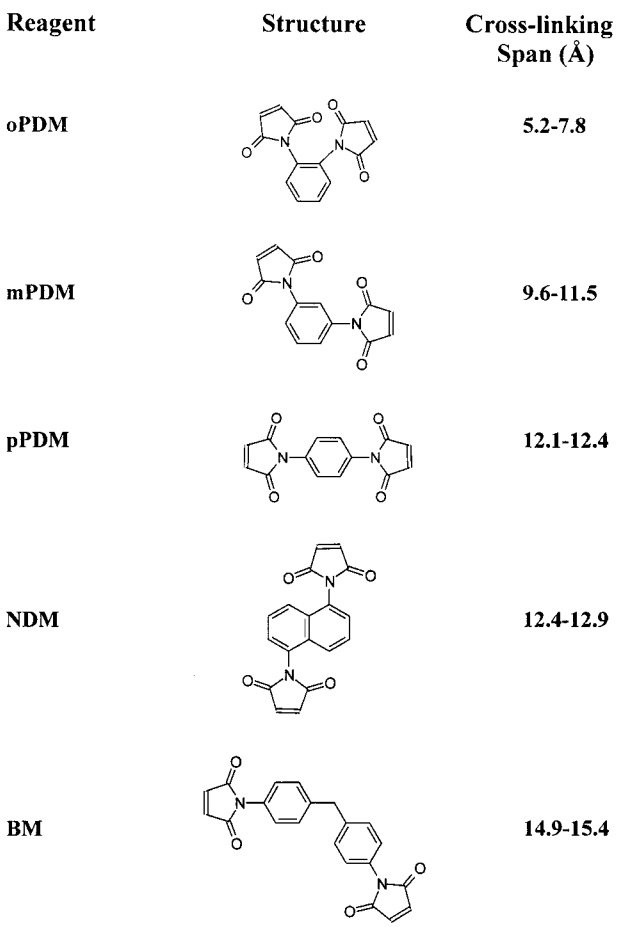

FIGURE 1: Chemical structures and cross-linking spans of the reagents utilized in this study. The structures were drawn in ChemDraw and transferred to the MacroModel program. The ranges of distances given for each reagent reflect the possible attachments of the sulfhydryls to the maleimide group in the different conformers of the reagents.

were monitored by measuring the Ca^{2+}- and EDTA-ATPase activities. In the second step, after SH1 was modified, the excess reagent was removed from the mixtures. The reaction mixtures were applied to Sephadex G-50 spin columns, which were equilibrated with 10 mM KCl, 10 mM imidazole, pH 7.0. Excess reagent was removed by centrifugation, and the samples were equilibrated to 25 °C. In the third step, the cross-linking reaction was monitored. After splitting the reaction mixture into two equal samples, nucleotide (1.0 mM MgADP, 1.0 mM MgATPγS, or 3.0 mM MgATP) was added to one of the samples while the other sample was used to monitor the cross-linking reaction without nucleotide. The reaction was quenched with 1.0 mM DTT in aliquots taken at various time points, and Ca^{2+}- and EDTA-ATPase activities of each time point were measured. Because of protein dilutions involved in these assays, the final concentrations of nucleotides carried over from the cross-linking reactions to the activity assays were 10 μM MgADP and MgATPγS and 30 μM MgATP. Although these levels of Mg^{2+} inhibited somewhat the Ca^{2+}- and EDTA-ATPase activities (data not shown), they did not complicate the determination of these activities. The ATPase activities were analyzed to calculate the cross-linking rates for all the reagents.

Rates of SH2 Modification. SH1 was modified by addition of 5-fold excess of NEM over S1 (20−25 μM). After 90

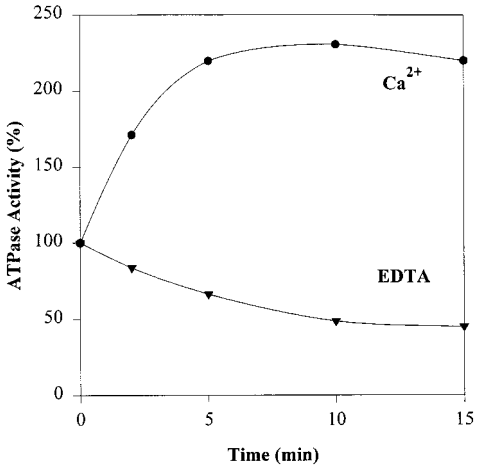

FIGURE 2: oPDM modification of S1. Ca^{2+}- (●) and EDTA- (▼) ATPase activities of samples taken at various time points were measured and plotted as a function of time. For oPDM modifications only, 1.0 mM MgADP was added to increase the rate of SH1 modification. As seen from this plot, the time chosen for maximal separation between Ca^{2+}- and EDTA-ATPases in this experiment was 10 min.

min, the reaction was terminated with the addition of 1.0 mM DTT. All SH1 modification reactions were carried out in 10 mM KCl, 10 mM imidazole, pH 7.0 at 4 °C. Ca^{2+}- and EDTA-ATPase activities were measured to determine the extent of SH1 modification. Under these conditions, 95−98% of the SH1 groups were modified (data not shown). SH1−NEM S1 was then dialyzed overnight in 10 mM KCl, 10 mM imidazole, pH 7.0, to remove excess reagent and DTT. SH2 was modified by the addition of 4-fold excess of cross-linking reagent (oPDM, mPDM, pPDM, NDM, BM in dimethylformamide) to S1 (10 μM). The modification reactions were performed at 25 °C in the absence or presence of 1.0 mM MgADP or 1.0 mM MgATPγS. To prevent aggregation, 0.2 M sucrose was added to the solutions. At various time points, the reaction was quenched in aliquots with 1.0 mM DTT, and the Ca^{2+}-ATPase activity of each sample was measured to monitor the extent of SH2 modification. As SH2 was modified, the Ca^{2+}-ATPase of S1 decreased. The rates of SH2 modification were determined from semilogarithmic plots of Ca^{2+}-ATPase activities of the modified samples versus reaction time.

RESULTS

Cross-Linking Rate Determination. To ascertain the kinetic effect of nucleotides on the SH1−SH2 cross-linking of S1, a method was devised to directly measure the cross-linking rates. Results of the oPDM reaction with S1 are presented in Figures 2 and 3 as representative of reactions with all the cross-linking reagents. Initially, an SH1-modification reaction profile was determined for each cross-linking reagent (Figure 2). Conditions (pH 7.0, 4 °C, 10 min for oPDM) were optimized to promote SH1 modification without significant SH2 cross-linking or monofunctional labeling of SH2. According to established procedures (*16*), the modification reaction was monitored by measuring the Ca^{2+}- and EDTA-ATPase activities of S1. As SH1 is modified, the Ca^{2+}-ATPase activity increases, and the EDTA-ATPase activity decreases (Figure 2). When the rate of SH1 modification slows down, the Ca^{2+}-ATPase begins to plateau

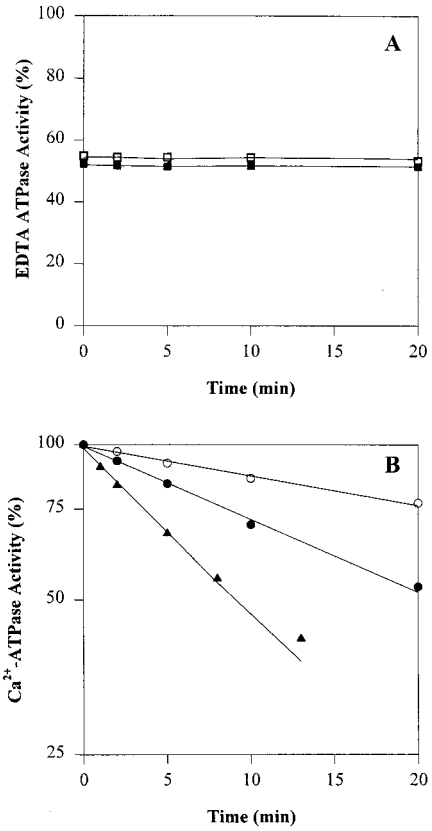

FIGURE 3: ATPase activity of S1 after the removal of excess oPDM. (A) EDTA-ATPase (□, ■); (B) Ca^{2+}-ATPase (○, ●, ▲); activities of S1 cross-linked in the absence (□, ○) and presence of 1.0 mM MgADP (■, ●) and 1.0 mM MgATPγS (▲). After the removal of excess reagent, samples were taken at various time points, and ATPase assays were performed to determine the cross-linking rate. EDTA-ATPase remains unchanged (A), indicating that the removal of excess oPDM was complete. The EDTA-ATPase for the sample with MgADP was displaced for graphical purposes. Semilogarithmic plots of Ca^{2+}-ATPase (B) show the decrease in this activity as a result of cross-linking. Addition of MgADP increased the rate of cross-linking by 2-fold. For MgATPγS, the increase in cross-linking was 7-fold.

and then decreases (due to SH2 cross-linking). The EDTA-ATPase activity also begins to level off. At this time, at the plateau of the Ca^{2+}-ATPase, the separation between the levels of Ca^{2+}-ATPase and EDTA-ATPase activities is largest and provides the greatest range for monitoring the cross-linking reaction. Once the time of maximal separation was established for each reagent, the reaction was carried out for that time and then excess reagent was removed quickly by centrifugation of the reaction mixtures on spin columns. Subsequently, Ca^{2+}- and EDTA-ATPase activities were measured to monitor the cross-linking reactions.

To determine the cross-linking rates, the ATPase activities were analyzed in detail as shown for the oPDM reaction with S1. The EDTA-ATPase assay measures only the activity of unlabeled S1 in either the unmodified or the modified S1 samples. The plot of the EDTA-ATPase activity versus time after removal of excess reagent shows no change in activity, indicating that there is no new modification occurring at either SH1 or SH2 on unlabeled S1 (Figure 3A). Therefore, the removal of excess reagent was complete. From the EDTA-ATPase, which is a linear function of unlabeled S1, the fraction of unlabeled S1 in the modified sample can be determined. By comparing the EDTA-ATPase activity of

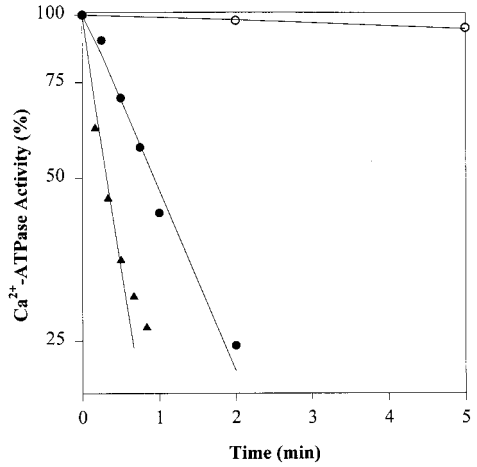

FIGURE 4: Semilogarithmic plots of pPDM cross-linking of S1 versus time. The cross-linking reactions were monitored in the absence (○) and presence of 1.0 mM MgADP (●) or 1.0 mM MgATPγS (▲). Addition of MgADP increased the rate of cross-linking ~54-fold. In the presence of MgATPγS, the rate increase was ~264-fold.

unmodified S1 to that of the modified S1, the percentage of unlabeled S1 in the modified samples is calculated. In the example shown in Figure 3A, the EDTA-ATPase activity of the modified S1 was 54% that of the unmodified S1; i.e., the modified sample contained 54% unlabeled S1. This value is needed in the subsequent analysis of the Ca^{2+}-ATPase activity results.

The Ca^{2+}-ATPase activity assay measures the activity of both labeled and unlabeled S1. The percentage of unlabeled S1 in each sample has been calculated via the EDTA-ATPase assay. Thus, the Ca^{2+}-ATPase activity contributed by unlabeled S1 can be subtracted from the total Ca^{2+}-ATPase of the modified S1 sample. The remaining Ca^{2+}-ATPase is that of SH1-labeled S1. This activity decreases as a result of SH1−SH2 cross-linking. The first time point at which data for the cross-linking reaction were acquired was set arbitrarily as the zero time point. All subsequent data for this reaction were normalized to the zero time point. In Figure 3B, the corrected Ca^{2+}-ATPase activity is plotted in a semilogarithmic form as a function of time. As SH2 is modified due to cross-linking, the Ca^{2+}-ATPase activity decreases. Since no new modification is occurring, the changes observed in the Ca^{2+}-ATPase activity are due to the cross-linking reaction alone. The reaction follows a first-order process and yields the cross-linking rates for oPDM (Figure 3B). For this reagent, the cross-linking rate (k_2) in the absence of nucleotide is 0.010 min^{-1}, and the cross-linking rates (k_{2N}) in the presence of nucleotides are 0.02 and 0.07 min^{-1} for MgADP and MgATPγS, respectively.

Effect of Nucleotides on Cross-Linking Rates. Although pPDM is widely used for the cross-linking of SH1 and SH2 on myosin, the kinetics of this reaction have not been studied yet. The results of the pPDM cross-linking reaction at 25 °C are presented in Figure 4. In the absence of nucleotides, the cross-linking reaction was slow and was monitored over a 40 min time period. Only the initial two time points were shown in Figure 4 (upper curve), but all of the data points (not shown) were fitted well by the same curve ($k_2 = 0.013$ min^{-1}). When MgADP was added, the rate of cross-linking was increased greatly ($k_{2N} = 0.70$ min^{-1}). Addition of MgATPγS increased even more the cross-linking rate ($k_{2N} = 2.9$ min^{-1}). Thus, the rate of SH1−SH2 cross-linking increases in the presence of nucleotide, and the increase depends on the type of nucleotide bound at the active site. These experiments were repeated for all of the cross-linking reagents. The results for k_2 and k_{2N} rate constants are listed in Table 1. The k_2 values represent the rates of SH1−SH2 cross-linking in the absence of nucleotide. Although there were slight variations among the reagents, all of them appeared to have similar cross-linking rates, 0.012 ± 0.005 min^{-1}. The k_{2N} values represent the rates of SH1−SH2 cross-linking in the presence of nucleotide. For these experiments, the variations in the rates were much larger, especially for the very fast reactions. To account for reagent-dependent differences in the reactivity of SH2, the rate constant data for each reagent are presented also in the form of k_{2N}/k_2 ratios (Table 1), i.e., the ratios of the cross-linking rates in the presence of nucleotide over those in the absence of nucleotide. The k_{2N}/k_2 ratios reveal the effect that the binding of nucleotide has on the rate of SH1−SH2 cross-linking. For oPDM, MgADP accelerated the rate of SH1−SH2 cross-linking only 2-fold. The k_{2N}/k_2 ratios for the other reagents were higher, showing between 40- and 50-fold increase in the rate of SH1−SH2 cross-linking. In the MgATPγS experiment, the k_{2N}/k_2 ratio for oPDM was 7-fold. The ratios for the other reagents were much higher. The maximal acceleration of cross-linking rate constants by MgATPγS, approximately 260-fold, was obtained with pPDM.

Table 1: Cross-Linking Rates[a] in the Presence and Absence of Nucleotides at 25 °C

reagent	k_2[b] (min^{-1})	k_{2N}[c] (min^{-1})	k_{2N}/k_2
	MgADP		
oPDM	0.010 ± 0.002	0.02 ± 0.01	2 ± 1
mPDM	0.017 ± 0.003	0.64 ± 0.02	38 ± 8
pPDM	0.013 ± 0.001	0.70 ± 0.05	54 ± 8
NDM	0.007 ± 0.001	0.35 ± 0.03	50 ± 11
BM	0.017 ± 0.001	0.72 ± 0.01	42 ± 3
	MgATPγS		
oPDM	0.010 ± 0.002	0.072 ± 0.01	7 ± 2
mPDM	0.015 ± 0.002	1.57 ± 0.16	105 ± 25
pPDM	0.011 ± 0.001	2.9 ± 0.07	264 ± 30
NDM	0.006 ± 0.001	1.15 ± 0.02	191 ± 33
BM	0.017 ± 0.004	1.36 ± 0.15	80 ± 28
	MgATP		
oPDM	0.009 ± 0.001	0.017 ± 0.001	2 ± 1
mPDM	0.014 ± 0.003	0.42 ± 0.05	30 ± 10
pPDM	0.010 ± 0.002	0.42 ± 0.04	42 ± 12
NDM	0.008 ± 0.001	0.33 ± 0.03	32 ± 8
BM	0.015 ± 0.003	0.37 ± 0.05	25 ± 8

[a] All rates were determined from semi-logarithmic plots of Ca^{2+}-ATPase activity of modified S1 cross-linking time similar to that shown in Figure 4. Each rate is the mean value of at least three independent experiments. [b] Rate of cross-linking in the absence of nucleotide. [c] Rate of cross-linking in the presence of 1.0 mM MgADP and MgATPγS or 3.0 mM MgATP.

In an attempt to examine the MgADP·P_i state, the cross-linking rates were also measured in the presence of MgATP. At 25 °C, MgATP yields a mixture of nucleotide states, dominated primarily by the MgADP·P_i state (*17*, *18*). Results shown in Table 1 indicate that the ratios of cross-linking rates in the presence over those in the absence of MgATP (k_{2N}/k_N) are smaller than those observed for MgADP. Importantly, S1 modification at SH1 redistributes the popula-

Table 2: SH2 Modification Rates[a] in the Presence and Absence of Nucleotides at 25 °C

reagent	k_2[b] (min^{-1})	k_{2N}[c] (min^{-1})	k_{2N}/k_2
		MgADP	
oPDM	0.007 ± 0.0005	0.025 ± 0.002	3.6 ± 0.5
mPDM, pPDM, NDM, BM	0.031 ± 0.014	0.133 ± 0.030	4.3 ± 1.9
		MgATPγS	
oPDM	0.007 ± 0.0005	0.038 ± 0.005	5.4 ± 1.1
mPDM, pPDM, NDM, BM	0.031 ± 0.014	0.230 ± 0.070	7.4 ± 3.3

[a] All rates were obtained from semi-logarithmic plots of the Ca^{2+}-ATPase activity of modified S1 versus time of reaction. The rates are the mean values of at least two independent experiments for each reagent. For mPDM, pPDM, NDM, and BM, the rates were similar and are, therefore, the mean values for the four reagents. [b] Rate of SH2 modification in the absence of nucleotide. [c] Rate of SH2 modification in the presence of 1.0 mM nucleotide.

tion of transition states toward the MgATP state (*19*). Clearly, without such information for the reagents used in this study, it is difficult to determine how much each of these states contributes to the overall effect on the cross-linking. However, in view of such redistribution of states, for the ratios obtained in the MgATP experiments to be smaller than those seen in both the MgATPγS and MgADP states, the MgADP•P_i state must either inhibit or have no effect on the SH1−SH2 cross-linking.

SH2 Modification Reaction. To test for any potential differences in the reactivity of the reagents toward SH2 in the presence of nucleotides (MgADP or MgATPγS), monofunctional labeling of SH2 was examined as well. The rate of SH2 modification was measured by preblocking SH1 with NEM and then following the modification of SH2 for each reagent. The results of these experiments are presented in Table 2. The rate of SH2 modification (k_2) for oPDM was 0.007 min^{-1}. For the other reagents, the rates (k_2) were approximately 0.03 min^{-1}, and there was little variation among the individual reagents. In the presence of nucleotide, the rate of SH2 modification (k_{2N}) by oPDM increased to 0.025 min^{-1} for MgADP and 0.038 min^{-1} for MgATPγS. For the other reagents, the rates (k_{2N}) were also increased in the presence of nucleotide, to 0.133 min^{-1} for MgADP and 0.230 min^{-1} for MgATPγS. Although the individual rates for oPDM and all the other reagents were different, the ratios of rates (k_{2N}/k_2) were similar for all of the reagents (3−4-fold for MgADP and 5−7-fold for MgATPγS.

DISCUSSION

It has been shown in previous studies on SH1 and SH2 that the binding of nucleotide to S1 accelerates both the modification and cross-linking of these two cysteines (*6*−*9*, *11*, *12*, *20*). Reagents with spans of up to 14 Å and down to 3 Å were used to cross-link SH1 to SH2. It is even possible for SH1 and SH2 to come close enough to one another to form a disulfide bond (*9*). However, for this disulfide bond formation to occur, nucleotides must be present and the reaction requires a time span of 24 h or more. Cross-linking with shorter reagents such as F_2DNB (1,5-difluoro-2,4-dinitrobenzene) also requires the presence of nucleotides and long reaction times (*7*, *8*). Because no systematic method of evaluating the rates of cross-linking reactions has been used so far, these reactions may be sampling infrequent, extreme, and low probability conformations of the helix.

From the crystal structure of S1, SH1 and SH2 are calculated to be approximately 19 Å apart. To accommodate for the above cross-linking reactions, the SH1−SH2 helix must be undergoing drastic changes. At least two speculative explanations can be suggested to describe what might be occurring in the helix. The helix or a part of it may be melting upon nucleotide binding, allowing SH1 and SH2 to approach each other. Alternatively, the helix may have increased flexibility in the presence of nucleotides. This increased flexibility could possibly be caused by rotations about glycine residues (699, 703, and 710) present in the sequence of the SH1−SH2 helix. Kinose et al. (*21*) and Patterson et al. (*22*) have recently shown that a mutation of the Gly699 residue (Gly680 in *Dictyostelium discoideum* myosin) severely hinders the motor function of myosin. This conserved residue is therefore necessary and may be required to maintain the rotational flexibility of the helix. The goal of this work was to explore the events occurring in the SH1−SH2 helix by kinetic analysis of the cross-linking of these cysteine groups.

Methodological Considerations. In this study, a new approach was taken to examine the cross-linking of SH1 and SH2. By isolating the cross-linking event, it was possible to determine what kinetic effect the nucleotides had on SH1−SH2 cross-linking. Several maleimide-based cross-linking reagents of different spans (5−15 Å) were used, allowing us to probe the distances separating SH1 and SH2 and to determine how the distances changed upon nucleotide binding.

One concern in the experiments was to minimize the possibility of monofunctional SH2 labeling. Several measures were taken to eliminate such a possibility. These include low temperature (4 °C), lower pH (pH 7.0), and low molar ratio of reagent to S1 (1.5:1.0). Until SH1 is labeled, the SH2 group under such conditions is not accessible to most reagents, including phenylmaleimide, a monfunctional equivalent of the dimaleimide cross-linking reagents (*12*, *23*, *24*). Any monofunctional SH2 labeling on S1 carrying a cross-linking reagent attached to SH1 was unlikely because of the rapid removal of excess reagent and the relatively slow rates of such labeling (Table 2). However, even if it occurs to some extent, such labeling, as well as the SH1−SH2 cross-linking completed prior to the first assay point of the cross-linking reaction, would be inconsequential to the subsequent kinetic analysis of the cross-linking. S1 labeled at both SH1 and SH2 and the cross-linked S1 have no ATPase activity. Thus, after correction of the activity for the contribution due to the unlabeled S1, the remaining Ca^{2+}-ATPase represented only SH1-labeled S1, and changes in the Ca^{2+}-ATPase were a result of the SH1−SH2 cross-linking. From experiment to experiment, the population of SH1-labeled S1 available for monitoring the SH1−SH2 cross-linking varied from 30 to 50%. However, the cross-linking rates determined from such different experiments were reproducible irrespective of the fraction of SH1-labeled S1. The data acquired from this study can be used to describe the changes in the SH1−SH2 helix due to nucleotide binding.

Significance of SH1−SH2 Cross-Linking Rates. As expected, our results show that the addition of nucleotide to

the SH1−SH2 cross-linking reactions increases the rate of such reactions. The increases, however, depended on the reagent used. This can be attributed to either the different spans of the reagents or the differing reactivities of the reagents toward SH2 in the presence of nucleotide. To ensure that the effects of nucleotide were due to the reagent span and not the reactivity, the rate of SH2 modification was determined for each reagent. The individual rates in the presence and absence of nucleotides (MgADP or MgATPγS) differed for oPDM and the other reagents, but the effect of nucleotide on the rates on SH2 labeling was similar for all of the reagents. This important conclusion is documented by the k_{2N}/k_2 ratios shown in Table 2, which reveal very little if any reagent-dependent variation for the SH2 labeling. In contrast to that, the k_{2N}/k_2 ratios determined for the SH1−SH2 cross-linking depend strongly on the reagent length (Table 1). The ratio representation of cross-linking rates factors out any differences in SH2 reactivities toward reagents and corrects for experimental variation in the three-step cross-linking reaction.

The overall picture emerging from k_2 data in Table 1 is that of S1 equilibrium between multiple states of the SH1−SH2 helix, with a relatively low probability for the states corresponding to any of the distances probed by the bifunctional reagents (5−15 Å). As judged from k_{2N} data, nucleotides cause a dramatic shift in these equilibria, increasing drastically the population of helix states covering SH1−SH2 distances between 9 and 15 Å. Thus, results presented in the form of k_{2N}/k_2 ratios are indicative of changes in the population of helix states (i.e., distances between SH1 and SH2) as a result of nucleotide binding.

Bar plots of the ratios of rates are shown in Figure 5 as a function of cross-linking spans of the bifunctional reagents. From these plots, it is clear that certain distances between SH1 and SH2 are preferred in the nucleotide-bound states. With MgADP, the ratios indicate that the distances between 9 and 15 Å are more populated than distances below 9 Å. For MgATPγS, the population of distances below 9 Å remains relatively small while the distances above 9 Å are even more populated. Moreover, in the presence of MgATPγS, the helix dynamics are such that a clear and dominant center of population of distances between SH1 and SH2 appears at around 12 Å.

A bar plot for k_{2N}/k_2 ratios is not shown for reactions in the presence of MgATP. Although the low values of these ratios and the likely presence of a significant MgATP-like state in the SH1-modified S1 (*19*, *25*) suggest little acceleration, if not inhibition, of the SH1−SH2 cross-linking in the MgADP·P_i state, these data cannot be resolved into specific nucleotide-state contributions. Ideally, complexes of MgADP with phosphate analogues (BeF_x, AlF_4^-, VO_4) could be used to study the S1 stabilized in a specific transition state (*26*−*28*). This is not possible in the experiments reported above because the kinetic analysis of the reactions depends on the ability to measure the ATPase activities, which are inhibited in the presence of these analogues. Another complication of these analogues is the slow formation of stable complexes with S1·MgADP, slower than most of the SH1−SH2 cross-linkings. Thus, the approach taken in this work, that of separating the cross-linking from the initial SH1 labeling, cannot be adopted to the complexes of S1·MgADP and phosphate analogues.

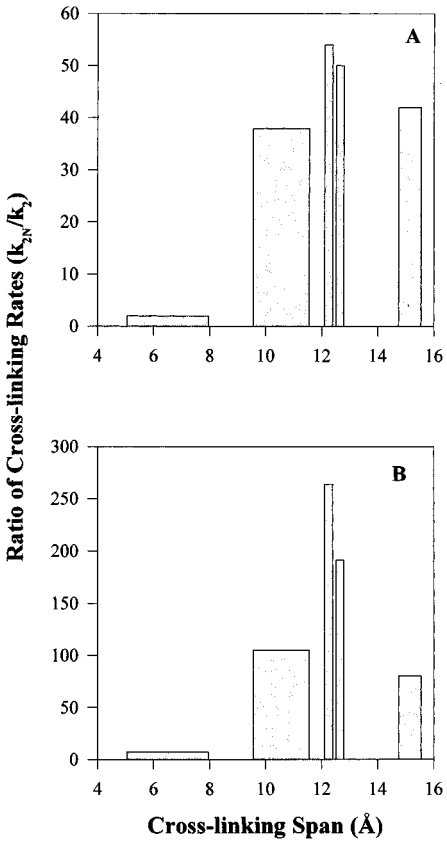

FIGURE 5: Ratios of cross-linking rates (k_{2N}/k_2) plotted as a function of cross-linking span of the different reagents. (A) Effect of MgADP; (B) effect of MgATPγS on the cross-linking reaction. k_2 and k_{2N} are the rates of cross-linking in the absence or presence of 1.0 mM nucleotide (MgADP or MgATPγS). The effect of MgADP on the rate of cross-linking for oPDM was only 2-fold while the increases for the reagents longer than 9 Å were approximately 40−50-fold. The effect of MgATPγS on the rate of cross-linking for oPDM was 7-fold. For the longer reagents, the increases were much greater, ranging from approximately 80−270-fold.

Implications. To determine the cross-linking rates of SH1 and SH2, it is necessary to first place the cross-linking reagent on SH1. Thus, the observed effects of nucleotides on the cross-linking rates actually represent changes occurring in the SH1-modified S1. Because the attachment of probes to SH1 alters the enzymatic and motor activities of S1 (*29*−*31*), questions may be raised about the effects of these probes on the SH1−SH2 helix. There is significant evidence to indicate that SH1 modification does not denature or alter drastically the SH1−SH2 helix. This includes the observation of the nucleotide-specific changes in the fluorescence of SH1-attached probes (*32*) and in the reactivity of SH2 on SH1-labeled S1 (this work). Also, the weakly and strongly bound acto-S1 states are described by similar equilibrium binding constants for the labeled and unlabeled S1 (*30*), and actin accelerates the release of phosphate analogues from both proteins (*20*, *32*), albeit not to the same extent. Clearly, important aspects of the communication between the ATP and actin sites on S1 are little changed by the SH1 labeling. Thus, we believe that nucleotide-induced shifts in the equilibria among different SH1−SH2 helix states are perhaps modulated by SH1 labeling but do occur also in unlabeled S1. According to this view, that SH1 labeling does not disrupt greatly the SH1−SH2 helix, the inhibition of the motor function and the actomyosin ATPase by SH1 modi-

fications would arise from the uncoupling of the helix from structural elements of S1 involved in these functions.

There may be several reasons why different states of the helix are not visualized in the X-ray structures of S1dC (*2*, *3*, *10*). Among them could be different flexibilities of this helix (because of different interactions with other structural elements in rabbit and *Dictyostelium* S1), the effect of the lever arm truncation in S1dC on the cysteine helix, and the trapping of a particular helix state by the crystallization process. Assuming that the lever arm of S1 can be viewed as a rigid body (obviously a simplification), the multiple states of the helix, which require its pivoting around glycine residues, would result in variable orientations of the lever arm with respect to the catalytic domain (*33*). The disordered state of S1 weakly bound to actin, frequently observed in structural and spectroscopic studies, may be a simple reflection of that effect. A discussion of possible implications of such transitions in the SH1−SH2 helix and the lever arm to the cross-bridge cycle must await a better analysis of the helix in the S1·ADP·P_i state, as well as information on its dynamic properties in the ternary complex of S1 with actin and MgADP. Such experiments and simulations of lever arm states as a function of SH1−SH2 helix transitions are part of the subsequent studies.

ACKNOWLEDGMENT

We thank Dr. Miguel Garcia-Garibay for his help with the cross-linking span determinations and Dr. Andrey Bobkov for his many helpful discussions.

REFERENCES

1. Bagshaw, C. R., and Trentham, D. R. (1975) *J. Supramol. Struct. 3*, 315−322.
2. Fisher, A., Smith, C., Thoden, J., Smith, R., Sutoh, K., Holden, H., and Rayment, I. (1995) *Biochemistry 34*, 8960−8972.
3. Gulick, A. M., Bauer, C. B., Thoden, J. B., and Rayment, I. (1997) *Biochemistry 36*, 11619−11628.
4. Smith, C. A., and Rayment, I. (1996) *Biochemistry 35*, 5404−5417.
5. Rayment, I. (1996) *J. Biol. Chem. 271*, 15850−15853.
6. Reisler, E., Burke, M., Himmelfarb, S., and Harrington, W. F. (1974) *Biochemistry 13*, 3837−3840.
7. Burke, M., and Reisler, E. (1977) *Biochemistry 16*, 5559−5563.
8. Wells, J. A., Knoeber, C., Sheldon, M. C., Werber, M. M., and Yount, R. G. (1980) *J. Biol. Chem. 255*, 11135−11140.
9. Wells, J. A., and Yount, R. G. (1980) *Biochemistry 19*, 1711−1717.
10. Rayment, I., Rypniewski, W., Schmidt-Base, K., Smith, R., Tomchick, D., Benning, M., Winkelmann, D., Wesenberg, G., and Holden, H. (1993) *Science 261*, 50−58.
11. Miller, L., Coppedge, J., and Reisler, E. (1982) *Biochem. Biophys. Res. Commun. 106*, 117−122.
12. Polosukhina, K., and Highsmith, S. (1997) *Biochemistry 36*, 11952−11958.
13. Godfrey, J. E., and Harrington, W. F. (1970) *Biochemistry 9*, 886−895.
14. Weeds, A., and Pope, B. (1977) *J. Mol. Biol. 111*, 129−157.
15. Fiske, C. H., and Subbarow, Y. (1925) *J. Biol. Chem. 60*, 375−400.
16. Sekine, T., Barnett, L. M., and Kielley, W. W. (1962) *J. Biol. Chem. 237*, 2769−2772.
17. Trentham, D. R., Eccleston, J. F., and Bagshaw, C. R. (1976) *Q. Rev. Biophys. 9*, 217−281.
18. Cooke, R. (1997) *Physiol. Rev. 77*, 671−697.
19. Ostap, E. M., White, H. D., and Thomas, D. D. (1993) *Biochemistry 32*, 6712−6720.
20. Phan, B. C., Peyser, Y. M., Reisler, E., and Muhlrad, A. (1997) *Eur. J. Biochem. 243*, 636−642.
21. Kinose, F., Wang, S. X., Kidambi, U. S., Moncman, C. L., and Winkelmann, D. A. (1996) *J. Cell Biol. 134*, 895−909.
22. Patterson, B., Ruppel, K. M., Wu, Y., and Spudich, J. A. (1997) *J. Biol. Chem. 272*, 27612−27617.
23. Reisler, E. (1982) *Methods Enzymol. 85 Pt. B*, 84−93.
24. Xie, L., Li, W. X., Barnett, V. A., and Schoenberg, M. (1997) *Biophys. J. 72*, 858−865.
25. Sleep, J. A., Trybus, K. M., Johnson, K. A., and Taylor, E. W. (1981) *J. Muscle Res. Cell Motil. 2*, 373−399.
26. Goodno, C. C., and Taylor, E. W. (1982) *Proc. Natl. Acad. Sci. U.S.A. 79*, 21−25.
27. Phan, B. C., Faller, L. D., and Reisler, E. (1993) *Biochemistry 32*, 7712−7719.
28. Maruta, S., Henry, G. D., Sykes, B. D., and Ikebe, M. (1993) *J. Biol. Chem. 268*, 7093−7100.
29. Marriott, G., and Heidecker, M. (1996) *Biochemistry 35*, 3170−3174.
30. Bobkov, A. A., Bobkova, E. A., Homsher, E., and Reisler, E. (1997) *Biochemistry 36*, 7733−7738.
31. Root, D. D., and Reisler, E. (1992) *Biophys J. 63*, 730−740.
32. Phan, B. C., Cheung, P., Stafford, W. F., and Reisler, E. (1996) *Biophys. Chem. 59*, 341−349.
33. Burghardt, T. P., Garamszegi, S. P., Park, S., and Ajtai, K. (1998) *Biochemistry 37*, 8035−8047.

BI9817212